J. Chem. Thermodynamics 89 (2015) 98–103

Contents lists available at ScienceDirect

J. Chem. Thermodynamics

journal homepage: www.elsevier.com/locate/jct

Isobutane as a probe of the structure of 1-alkyl-3-methylimidazolium bis(trifluoromethylsulfonyl)imide ionic liquids

Laure Pison [a], Varinia Bernales [a,b,1], Patricio Fuentealba [c], Agilio A.H. Padua [a], Margarida F. Costa Gomes [a,*]

[a] Clermont Université, Université Blaise Pascal, Institut de Chimie de Clermont-Ferrand, UMR 6296 CNRS, équipe Thermodynamique et Interactions Moléculaires, ICCF-TIM, BP 80026, F-63171 Aubière, France
[b] Departamento de Química, Facultad de Ciencias, Universidad de Chile, Las Palmeras #3425, Ñuñoa, Casilla, 653-SCL Santiago, Chile
[c] Departamento de Física, Facultad de Ciencias, Universidad de Chile, Las Palmeras #3425, Ñuñoa, Casilla, 653-SCL Santiago, Chile

ARTICLE INFO

Article history:
Received 7 January 2015
Received in revised form 17 April 2015
Accepted 20 April 2015
Available online 7 May 2015

Keywords:
Gas solubility
1-Alkyl-3-methylimidazolium bis(trifluoro methylsulfonyl)imide ionic liquids
Isobutane
Methylpropane

ABSTRACT

An experimental study of the solubility and of the thermodynamic properties of solvation, between temperatures (303 and 343) K and at pressures close to atmospheric, of 2-methylpropane (isobutane) in several ionic liquids based on the bis(trifluoromethylsulfonyl)imide anion and on 1-alkyl-3-methylimidazolium cations, $[C_nC_1Im][NTf_2]$, with alkyl side-chains varying from two to ten carbon atoms is presented. The isobutane solubility increases with increasing size of the alkyl side-chain of the cation in the ionic liquid and decreases with increasing temperature (as typical of an exothermal dissolution process). The mole fraction solubility of isobutane varies from $0.904 \cdot 10^{-2}$ in $[C_2C_1Im][NTf_2]$ at $T = 343$ K to $1.002 \cdot 10^{-1}$ in $[C_{10}C_1Im][NTf_2]$ at $T = 303$ K. The values measured in this work are compared to the behaviour of n-butane in the same ionic liquids published in a previous study (Costa Gomes *et al.*, 2012). Isobutane was found to be significantly less soluble than n-butane in all the ionic liquids. The differences found are interpreted in relation to the molecular structures obtained by molecular dynamics simulations for the solutions of n-butane and isobutane in the studied $[C_nC_1Im][NTf_2]$ ionic liquids.

1. Introduction

Because ionic liquids can exist in a huge variety of cation–anion combinations and the ions interact in a sophisticated manner, it is important to understand, at a molecular level, the key factors determining the solubilisation of different classes of solutes. It has been shown, both by molecular simulation and experimentally, that many ionic liquids display medium range ordering with the co-existence of two types of nanoscale aggregates: one formed by the charged head-groups of the ions and the other by the non-polar side chains, which are most often part of the structure of the cation [1]. The solvation of different solutes will take place preferentially in one domain or the other, depending on the nature of their interactions (polar, nonpolar or associating) [1,2].

We have previously used different families of simple gaseous solutes, alkanes [3] or perfluoroalkanes [4], to probe the local structure and molecular interactions in solutions of ionic liquids based on alkylimidazolium [3] or tetraalkylphosphonium [4] cations. In both studies, it was shown that the nature of the ionic liquids, as nano-segregated fluids, must be taken into account to understand their ability to dissolve different gases, even when these are similar in molecular terms. In the case of gaseous perfluoroalkanes in tetraalkylphosphonium-based ionic liquids we have concluded that, depending on the size of the solute, the gas explores different domains of the ionic liquid structure. This behaviour explains the larger solubility of the solute interacting in a less favourable way with the solvent [4] and points towards complex mechanisms of solvation, event in the case of those relatively simple solutes. In fact, perfluoropropane, C_3F_8, is more soluble than perfluoromethane or perfluoroethane in the tetraalkylphosphonium-based ionic liquids even if the perfluorinated chains of the solute are not expected to interact favourably with the long alkyl chains of the cation.

In the case of the dissolution of alkanes in imidazolium-based ionic liquids, two conclusions could be upheld from previous studies [3]: larger gaseous alkanes are more soluble as they interact more favourably with the non-polar side chains; the gaseous solutes are more soluble in ionic liquids with longer alkyl-side chains because they are more mobile in the media and the solvation is entropically more favourable.

In order to understand fully the solubility of apolar solutes in ionic liquids with different relative sizes of polar and apolar

* Corresponding author.
E-mail address: Margarida.c.gomes@univ-bpclermont.fr (M.F. Costa Gomes).
[1] Present address: Department of Chemistry, Supercomputing Institute, and Chemical Theory Center, University of Minnesota, Minneapolis, MN 55455-0431, USA.

http://dx.doi.org/10.1016/j.jct.2015.04.026
0021-9614/

domains, in particular the relative importance of the enthalpy and entropy of solvation towards the solubility of alkanes (apolar solutes) in ionic liquids based on bis(trifluoromethylsulfonyl)imide anion and on 1-alkyl-3-methylimidazolium cations, $[C_1C_nIm][NTf_2]$, we have studied the solubility of 2-methylpropane (isobutane) in $[C_1C_nIm][NTf_2]$ ionic liquids with n varying from two to ten carbon atoms. The values determined herein can be compared to those for n-butane in the same family of ionic liquids and, with the help of molecular simulation, check the importance of the structure of the branched isomer on the gas solubility.

2. Experimental

2.1. Materials

The samples of 1-*n*-alkyl-3-methylimidazolium bis(trifluoromethylsulfonyl)imide ionic liquids (n = 2, 6, 8, 10) are the same used and characterised before [3] and were synthesised and purified at the QUILL Centre, Belfast, following a well-established procedure [5]. All the samples were washed thoroughly with water to remove the undesired LiCl salt formed in the reaction and any potential water-soluble impurity that might be present and that could affect the accuracy of the gas solubility measurements. The minimum mole fraction purity is of 0.99 as found by ^{1}H and ^{19}F NMR spectroscopy. The sample of 1-butyl-3-methylimidazolium bis(trifluoromethylsulfonyl)imide was synthesised and characterised at the University of Lyon following the procedures described in detail previously [6].

The ionic liquids were kept under vacuum for 15 h at T = 303 K before each measurement. The water contents of each degassed sample were determined, with an uncertainty of $\pm 5 \cdot 10^{-6}$, using a coulometric Karl Fisher titrator (Mettler Toledo DL31). The water content of the degassed samples was found lay between $50 \cdot 10^{-6}$ for $[C_4C_1im][NTf_2]$ up to $150 \cdot 10^{-6}$ for $[C_8C_1im][NTf_2]$. The source and purity of each one of the samples used are listed in table 1.

The gas used, 2-methyl propane, was supplied by Linde gas. The stated mole fraction purity is of 0.995 with impurities $C_nH_m \leqslant 5000 \cdot 10^{-6}$.

2.2. Solubility measurements

The experimental method used for the gas solubility measurements is based on an isochoric saturation technique and has been described in previous publications [7,8]. The quantity of degassed ionic liquid introduced in the equilibration cell is determined gravimetrically. This quantity is equal to the amount of solvent present in the liquid solution, n_1^{liq}, as the ionic liquid does not present a measurable vapour pressure. When the thermodynamic equilibrium is attained, the pressure above the liquid solution is constant and is directly related to the amount of solute present in the liquid solution, n_2^{liq} (subscripts 1 and 2 stand for solvent and solute, respectively). This amount of solute is calculated by the difference between two pVT measurements: first when the gas is introduced in a calibrated bulb with volume V_{GB} and second after thermodynamic equilibrium is reached:

TABLE 1
Origin, purity and water content of the ionic liquid samples used. The purity was determined by ^{1}H and ^{13}C NMR and the water content using a Coulometric Karl Fisher titrator.

Ionic liquid	Origin	Purity	Water content (ppm)
$[C_2C_1Im]$ $[NTf_2]$	QUILL, Belfast	0.99	64
$[C_4C_1Im]$ $[NTf_2]$	C2P2, Lyon	>0.99	50
$[C_6C_1Im]$ $[NTf_2]$	QUILL, Belfast	0.99	87
$[C_8C_1Im]$ $[NTf_2]$	QUILL, Belfast	0.99	150
$[C_{10}C_1Im]$ $[NTf_2]$	QUILL, Belfast	0.99	102

TABLE 2
Experimental values for the solubility of i-C_4H_{10} in $[C_nC_1Im][NTf_2]$ ionic liquids (n = 2, 4, 6, 8 and 10) expressed as gas mole fraction at the experimental pressure, x_{gas}, as Henry's law constants K_H, and as gas mole fraction corrected for a partial pressure of solute of 0.1 MPa, x_{gas}^{1bar}. p is the experimental equilibrium pressure and the per cent deviation is relative to the correlations of the data.

$\frac{T}{K}$	$\frac{p}{10^2 Pa}$	$\frac{x_{gas}}{10^{-2}}$	$\frac{K_H}{10^5 Pa}$	$\frac{x_{gas}^{1bar}}{10^{-2}}$	$\frac{dev}{\%}$
		i-C_4H_{10} + $[C_2C_1Im][NTf_2]$			
303.25	599.1	1.384	42.64	2.285	+0.6
303.26	624.0	1.436	42.76	2.279	+0.3
303.29	597.8	1.363	43.18	2.257	−0.6
313.26	627.5	1.136	54.43	1.794	−0.5
313.35	626.3	1.126	54.83	1.781	−1.0
323.25	654.8	0.935	69.01	1.418	−0.9
323.26	683.1	0.994	67.72	1.445	+1.0
323.31	652.4	0.960	67.02	1.460	+2.1
333.22	681.1	0.769	87.41	1.122	−1.4
333.35	679.6	0.777	86.33	1.136	+0.1
343.21	706.8	0.631	110.67	0.887	−2.1
343.23	738.4	0.689	105.72	0.929	+2.5
343.24	705.1	0.641	108.58	0.904	−0.1
		i-C_4H_{10} + $[C_6C_1Im][NTf_2]$			
303.18	577.3	3.338	17.04	5.720	−1.9
306.15	538.7	2.815	18.88	5.165	+1.8
313.17	560.0	2.511	22.01	4.438	+1.9
313.18	608.2	2.792	21.47	4.548	−0.6
323.16	637.2	2.361	26.61	3.677	−0.3
323.17	581.9	2.175	26.41	3.705	−1.1
333.11	616.2	1.849	32.91	2.979	+0.4
333.14	606.8	1.836	32.66	3.002	−0.5
333.15	665.0	2.002	32.78	2.991	−0.1
343.11	630.8	1.551	40.20	2.443	+0.3
343.12	691.4	1.719	39.71	2.473	−1.0
343.16	643.7	1.567	40.60	2.419	+1.2
		i-C_4H_{10} + $[C_4C_1Im][NTf_2]$			
303.17	555.1	2.149	25.46	3.827	−0.5
303.18	530.6	2.046	25.58	3.809	+0.0
313.18	583.8	1.742	33.06	2.954	−0.2
313.28	562.5	1.641	33.82	2.888	+1.8
323.18	610.9	1.420	42.46	2.305	−1.4
323.20	590.7	1.354	43.08	2.272	+0.0
333.19	637.3	1.146	54.90	1.786	−2.3
333.25	620.0	1.061	57.73	1.698	+2.5
343.18	662.7	0.918	71.32	1.377	−2.7
343.27	646.8	0.846	75.55	1.300	+2.8
		i-C_4H_{10} + $[C_8C_1Im][NTf_2]$			
303.17	556.9	4.586	11.97	8.142	−0.7
303.17	507.9	4.122	12.16	8.014	+0.9
313.16	543.1	3.425	15.66	6.238	+1.9
313.17	529.5	3.441	15.20	6.426	−1.1
313.18	531.9	3.474	15.12	6.460	−1.6
323.15	564.4	2.870	19.43	5.038	−0.4
323.16	575.8	2.860	19.88	4.921	+1.9
333.16	594.8	2.375	24.75	3.962	+0.4
333.17	592.8	2.420	24.21	4.050	−1.8
343.16	623.2	1.981	31.10	3.158	+0.4
		i-C_4H_{10} + $[C_{10}C_1Im][NTf_2]$			
303.24	530.8	5.386	9.721	10.02	−1.3
303.25	523.9	5.211	9.918	9.825	+0.7
303.25	519.3	5.181	9.889	9.854	+0.4
313.26	562.6	4.304	12.90	7.572	+1.0
313.26	558.7	4.328	12.74	7.667	−0.3
323.24	598.3	3.565	16.57	5.907	+1.3
323.25	594.7	3.641	16.12	6.069	−1.4
333.24	628.8	3.062	20.28	4.834	−2.1
333.25	631.4	2.966	21.03	4.663	+1.5
343.22	660.9	2.579	25.32	3.878	−2.4

Standard uncertainties of the measured quantities: $T \pm 0.01$ K; $p \pm 10$ Pa; 1.5% in x_{gas}; 1.5% in K_H.

$$n_2^{liq} = \frac{p_{ini} V_{GB}}{[Z_2(p_{ini}, T_{ini}) RT_{ini}]} - \frac{p_{eq}(V_{tot} - V_{liq})}{[Z_2(p_{eq}, T_{eq}) RT_{eq}]}, \quad (1)$$

where p_{ini} and T_{ini} are the pressure and temperature in the first pVT determination and p_{eq} and T_{eq} the pressure and temperature at the

TABLE 3
Parameters of equation (3) used to smooth the experimental results of K_H from table 2 along with the standard deviation of the fit *s*.

Ionic liquid	A_0	$\frac{A_1}{K}$	$\frac{A_2}{K^2}$	*s*
$[C_2C_1Im][NTf_2]$	+18.64	$-6.888 \cdot 10^3$	$+7.203 \cdot 10^5$	1.0
$[C_4C_1Im][NTf_2]$	+22.18	$-9.144 \cdot 10^3$	$+1.031 \cdot 10^6$	1.1
$[C_6C_1Im][NTf_2]$	+13.77	$-4.589 \cdot 10^3$	$+3.877 \cdot 10^5$	0.9
$[C_8C_1Im][NTf_2]$	+15.82	$-5.836 \cdot 10^3$	$+5.442 \cdot 10^5$	1.1
$[C_{10}C_1Im][NTf_2]$	+12.45	$-3.718 \cdot 10^3$	$+1.929 \cdot 10^5$	1.2

equilibrium. The V_{tot} is the total volume of the equilibration cell, V_{liq} is the volume of the liquid solution and Z_2 is the compression factor for the pure gas. The mole fraction solubility can be used to calculate the Henry's law constant:

$$K_H = \lim_{x_2 \to 0} \frac{f_2(p, T, x_2)}{x_2} \cong \frac{\phi_2(p_{eq}, T_{eq}) p_{eq}}{x_2}, \quad (2)$$

where f_2 is the fugacity of the solute and ϕ_2 its fugacity coefficient.

We consider that the volume of the ionic liquid does not change when the gas is solubilised and so the volume of the liquid solution is considered as equal to the molar volume of the pure ionic liquid. The molar volumes of the pure ionic liquids here were calculated from density measurements.

2.3. Molecular simulations

The ionic liquids were represented by all-atom force fields based on the OPLS_AA/AMBER framework [9,10] but with parameters developed specifically for the ions considered here [11,12]. The gases were modelled using OPLS-AA force field [12,13].

The ionic liquids were simulated in periodic cubic boxes containing 300 ion pairs of $[C_2C_1Im][NTf_2]$, or 250 ion pairs of $[C_6C_1Im][NTf_2]$ and $[C_{10}C_1Im][NTf_2]$, using the molecular dynamics method implemented in the DL_POLY package [9]. Initial low-density configurations, with ions placed at random, were equilibrated to attain liquid-like densities and structures at $T = 373$ K and 100 kPa. Temperature and pressure were maintained using a Nosé–Hoover thermostat and barostat, respectively. Once the equilibrium density attained, simulations runs of 400 ps were performed, with an explicit cutoff distance of 1.6 nm for non-bonded interactions, from which 2000 configurations were stored. Structural quantities such as radial and spatial distribution functions were calculated from configurations generated during the production runs. Additionally, simulation boxes containing 8 molecules of n-butane and 8 molecules of isobutane separately, in the ionic liquids, were prepared in the same manner, to calculate (solute + solvent) radial distribution functions between the gas and the ionic liquid and the (cation + anion) interaction energy in the presence of the solute molecules.

The total energy of the simulated systems containing solute and ionic liquid was decomposed into contributions from different pairs of species, in order to quantify the predominant interactions. For that, the energy of each configuration (same atomic coordinates) was recalculated taking into account only the relevant pairs

TABLE 4
Thermodynamic properties of isobutane and of n-butane [3] in $[C_nC_1Im][NTf_2]$ ionic liquids ($n = 2, 4, 6, 8, 10$), at $T = 303$ K.

Ionic liquid	$\Delta_{solv}H^\infty$ / kJ · mol^{-1}	$T\Delta_{solv}S^\infty$ / kJ · mol^{-1}
	i-C$_4$H$_{10}$	
$[C_2C_1Im][NTf_2]$	−17.9 ± 0.9	−27 ± 2
$[C_4C_1Im][NTf_2]$	−19.6 ± 0.9	−28 ± 2
$[C_6C_1Im][NTf_2]$	−17 ± 1	−24 ± 1
$[C_8C_1Im][NTf_2]$	−18.7 ± 0.5	−25.0 ± 0.9
$[C_{10}C_1Im][NTf_2]$	−20.2 ± 0.4	−26.0 ± 0.8
	n-C$_4$H$_{10}$[a]	
$[C_2C_1Im][NTf_2]$	−20.5 ± 0.7	−28.7 ± 0.4
$[C_4C_1Im][NTf_2]$	−20.4 ± 0.1	−27 ± 1
$[C_6C_1Im][NTf_2]$	−23 ± 1.5	−28.3 ± 0.9
$[C_8C_1Im][NTf_2]$	−20.9 ± 0.1	−26.2 ± 0.9
$[C_{10}C_1Im][NTf_2]$	−21.6 ± 0.1	−26.2 ± 0.9

[a] Values calculated from the data in reference [3].

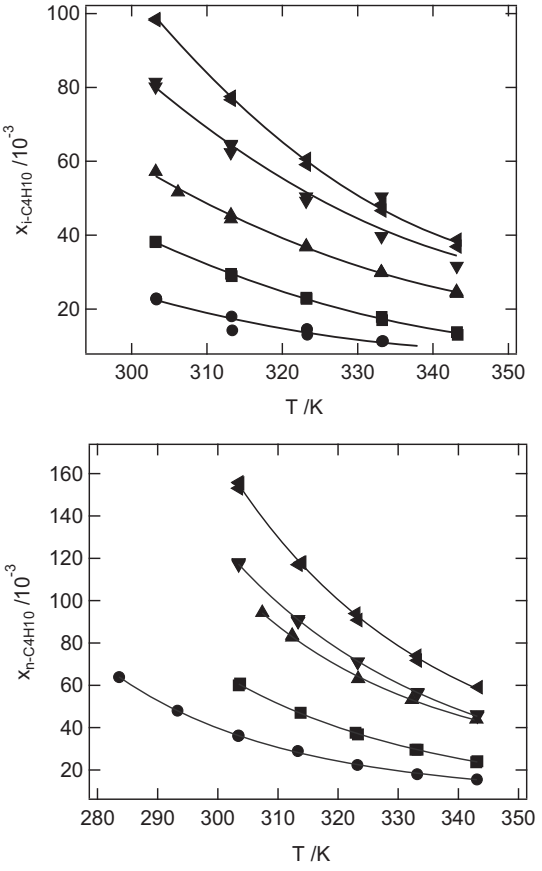

FIGURE 1. Plot of mole fraction solubility as a function of temperature and at a 100 kPa partial pressure of gas, of i-C_4H_{10} (top plot) and n-C_4H_{10} (bottom plot) in $[C_nC_1Im][NTf_2]$ ionic liquids: ●, $n = 2$; ■, $n = 4$; ▲, $n = 6$; ▼, $n = 8$; ◀, $n = 10$. The bottom plot represents the data published in reference [3].

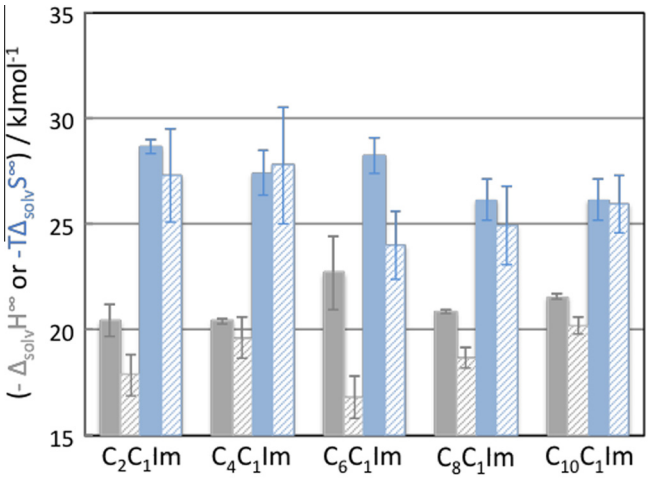

FIGURE 2. Enthalpy of solvation (in grey) and entropy of solvation (in blue) of n-butane (filled bars) and iso-butane (patterned bars) in the $[C_nC_1Im][NTf_2]$ ionic liquids studied, at $T = 303$ K. (For interpretation of the references to colour in this figure legend, the reader is referred to the web version of this article.)

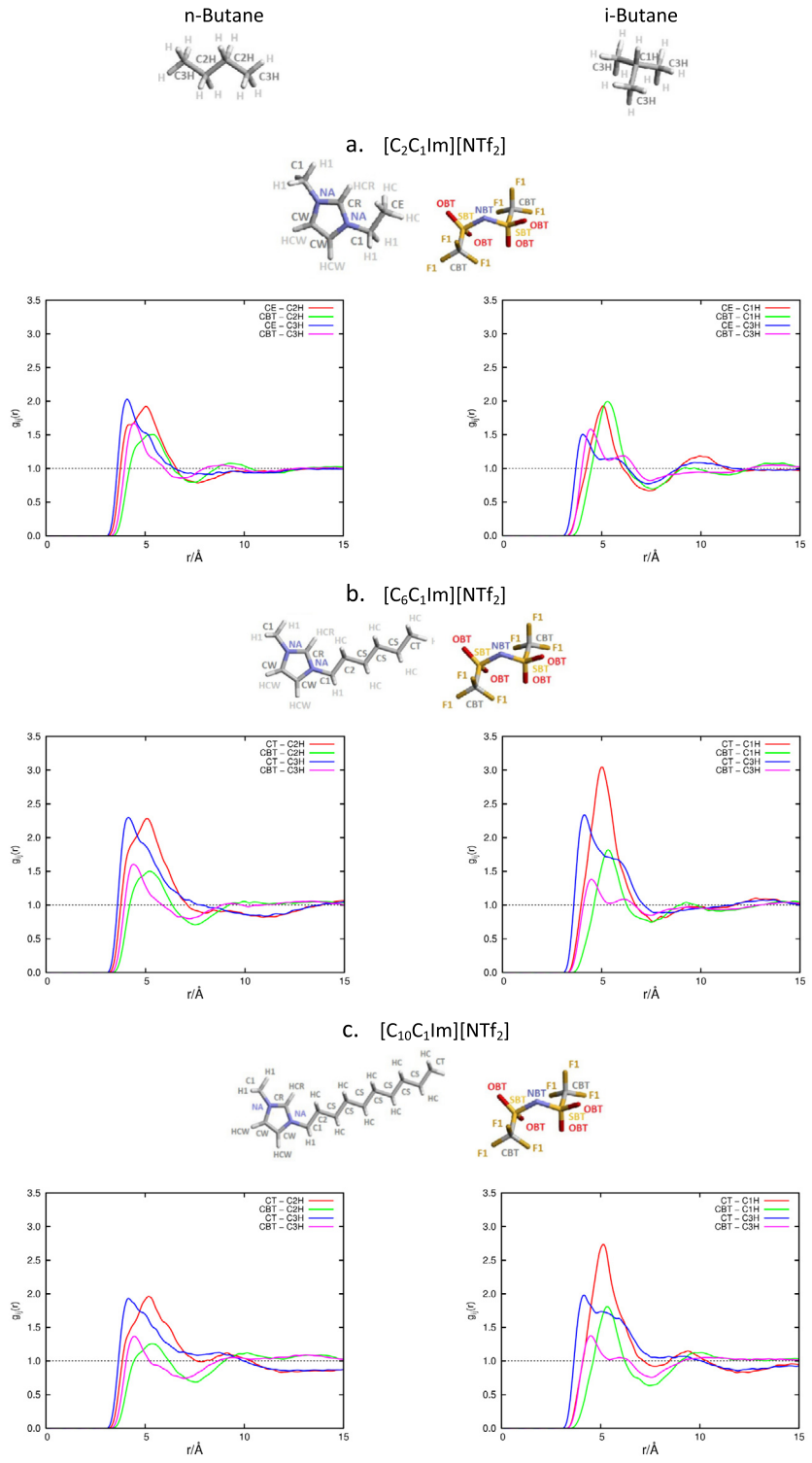

FIGURE 3. Site-site, (solute + solvent) radial distribution functions of n-butane (plots on the left-hand side) and iso-butane (plots on the right-hand side) for three of the ionic liquids studied: $[C_2C_1Im][NTf_2]$ (first row); $[C_6C_1Im][NTf_2]$ (second row) and $[C_{10}C_1Im][-NTf_2]$ (third row). The label along the *x*-axis should read as 10 *r*/nm.

of species, in turn. Also, the total energy was decomposed into intramolecular terms, short-range (Lennard-Jones) and electrostatic. In this manner, a detailed picture of the energetics of the system can be obtained.

3. Results and discussion

The densities of the ionic liquids, at atmospheric pressure and as a function of temperature, have been determined previously [3,6].

As in the case of the previous study for n-butane [3], multiple experimental data points were obtained for the solubility of isobutane in each ionic liquid in the temperature interval between (303 and 343) K in steps of approximately $T = 10$ K. The experimental mole fraction solubility of isobutane in $[C_nmim][NTf_2]$, with $n = 2$, 4, 6, 8 and 10 are reported in table 2. Henry's law constants can be calculated from the experimental values and are used to determine the mole fraction solubility assuming a partial pressure of the gaseous solute equal to 0.1 MPa. The second virial coefficients for

the gases, necessary for the calculation of the compressibility factor, were taken from the compilation by Dymond and Smith [14].

The Henry's law constants have been adjusted to an empirical equation of the form:

$$\ln\left[K_H/10^5\ \text{Pa}\right] = \sum_{i=0}^{n} A_i (T/\text{K})^{-i}. \quad (3)$$

The coefficients A_i as well as the standard deviations of the fits, considered as a measure of the precision of the experimental solubility data for the different gases in the five ionic liquids are listed in table 3. The Henry's law constants, calculated from the solubility measurements, are in general considered to be precise to within (1 to 2)%. The accuracy of the present results can be estimated from the comparison of the Henry's law constants calculated here with those measured and published by other authors. Camper *et al.* [15] have measured the solubility of isobutane in $[C_2C_1Im][NTf_2]$ and report a value for the Henry's law constant at 40 °C equal to 51.95 atm (or $52.64 \cdot 10^5$ Pa), 2.6% lower than the one determined in this work ($54.03 \cdot 10^5$ Pa).

The solubility of isobutane in all ionic liquids studied is depicted in figure 1 together with that, previously determined, of n-butane [3]. The solubility of n-butane is *circa* 1.6 times higher than that of iso-butane in all the ionic liquids studied and decreases with temperature, indicating that the process of dissolution of the gases is exothermic. The relative variation of the solubility of both gases with the length of alkyl side-chain of the cation is constant, the solubility increasing with the increase of the alkyl side-chains.

In order to determine the reasons behind the differences in solubility between the two gases, the thermodynamic properties of solvation were calculated. The variation with temperature of the solubility of the gases studied in the ionic liquids, expressed in Henry's law constant, can be used for the calculation of the thermodynamic properties of solvation [4]:

$$\Delta_{solv}G^{\infty} = RT\ln(K_H/p^0), \quad (4)$$

where p^0 is the standard-state pressure. The partial molar differences in enthalpy and entropy between the ideal gas and solution states can be obtained by calculating the corresponding partial derivatives of the Gibbs energy with respect to temperature

$$\Delta_{solv}H^{\infty} = -T^2\partial/\partial T(\Delta_{solv}G^{\infty}/T) = -RT^2\partial/\partial T\left[\ln\left(K_H/p^0\right)\right], \quad (5)$$

$$\begin{aligned}\Delta_{solv}S^{\infty} &= (\Delta_{solv}H^{\infty} - \Delta_{solv}G^{\infty})/T \\ &= -RT\partial/\partial T\left[\ln\left(K_H/p^0\right)\right] - R\ln\left(K_H/p^0\right). \end{aligned} \quad (6)$$

The values of the thermodynamic properties of solvation in the temperature range covered in this work for iso-butane and those previously published for n-butane [3] are listed in table 4 and represented in figure 2.

The enthalpy of solvation for isobutane is always lower than that of n-butane in the ionic liquids studied, a fact that explains the higher solubility of the latter gas. Although the solubility of isobutane increases when the alkyl side-chain of the imidazolium cation increases, this behaviour cannot easily be rationalised by the analysis of the thermodynamic properties of solvation. As can be observed in figure 2, there are two distinct patterns in the behaviour of the thermodynamic properties of solvation for isobutane in the $[C_nC_1Im][NTf_2]$ ionic liquids: one for $n = 2$, 4 and another for $n \geqslant 6$. In both groups the solubility of the solute increases because the enthalpy of solution becomes more negative and the entropy of solvation slightly more positive. This behaviour is different from that observed for n-butane for which the enthalpy of solvation remained approximately constant for all the ionic liquids, the increase of the gas solubility with the increase of the alkyl side-chain of the cation being explained in that case by more favourable entropies of solvation.

The molecular structure of these mixtures was studied by molecular simulation by calculating all the site-site (solute + solvent) radial distribution functions (RDFs) for the solutions of iso-butane in $[C_2C_1Im][NTf_2]$, $[C_6C_1Im][NTf_2]$ and $[C_{10}C_1Im][NTf_2]$. As can be seen in figure 3, where some of the most significant (solute + solvent) RDFs are plotted, the differences between the structure of the n-butane and the iso-butane solutions depend on the ionic liquid.

For $[C_2C_1Im][NTf_2]$, the most striking difference is found on the probability of finding the $-CF_3$ group of the NTf_2^- anion near the solute. The anion has a larger probability of being found near iso-butane than near n-butane when each solute is dissolved in $[C_2C_1Im][NTf_2]$. This effect is also found to a lesser extend for iso-butane dissolved in $[C_6C_1Im][NTf_2]$ and $[C_{10}C_1Im][NTf_2]$ but, in those cases, the most noticeable difference is the much larger probability of finding the terminal carbon atom of the alkyl side-chain of the cation near the central carbon atoms of the solute.

These differences in the structure of the solutions are in agreement with the thermodynamic properties of solvation found

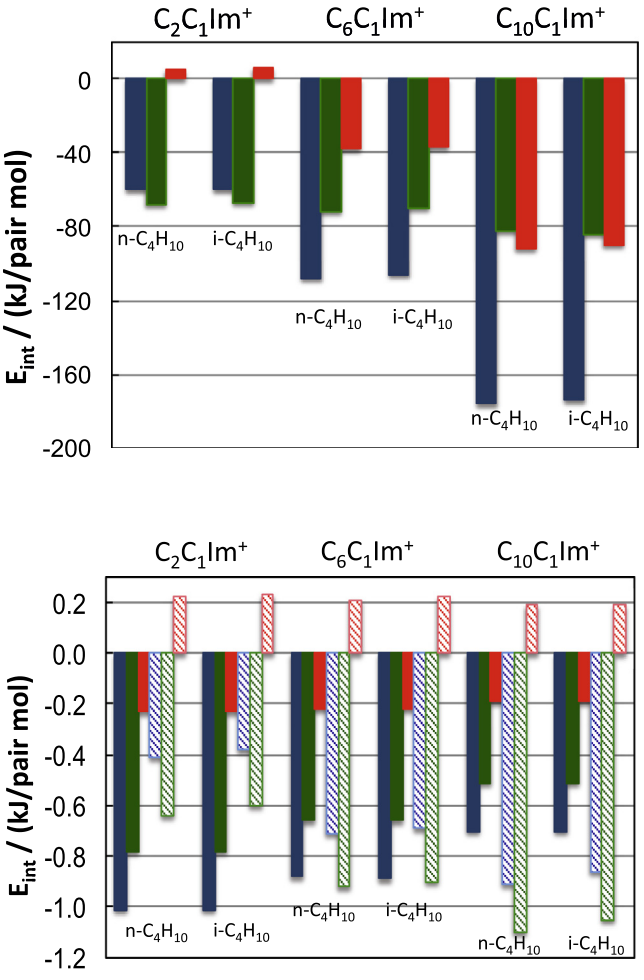

FIGURE 4. Energy decomposition calculated by molecular simulation. In blue, the total potential energy; in green, the dispersion interaction energy; and in red, the electrostatic contribution to the interaction energy. Upper plot: (cation + anion) interaction energy for the three ionic liquids $[C_2C_1Im][NTf_2]$, $[C_6C_1Im][NTf_2]$ and $[C_{10}C_1Im][NTf_2]$ in the presence of the two solutes n-C_4H_{10} and i-C_4H_{10}. Lower plot: (solute + ionic liquid) interaction energies for the three ionic liquids. The filled bars represent the (solute + anion) interaction energy, and the patterned bars represent the (solute + cation) interaction energy. (For interpretation of the references to colour in this figure legend, the reader is referred to the web version of this article.)

experimentally. The more negative enthalpies of solvation found for isobutane in the ionic liquids with longer alkyl side-chains would correspond to a more favourable interaction between the terminal carbons of the alkyl chain of the cation and the solute.

The overall system configuration energy calculated by molecular simulation was decomposed into the energies between each pair of species, as represented in figure 4. In the upper plot, no marked differences are observed between the dispersion and electrostatic contributions to the total potential energy of the solutions of butane and isobutane in the ionic liquids. In the lower plot, on the other hand, important differences can be observed between the interaction energies of n-butane and isobutane and the cations of the ionic liquids, this interaction becoming more favourable for the ionic liquids with a larger alkyl side-chain. It can be observed that the electrostatic interactions between the solutes and the ionic liquids remain approximately constant while the dispersion contribution to the energy become for significant for the ionic liquids with the large cations. It is noticeable that this term of the energy is always more negative for n-butane than for iso-butane, a fact that explains the experimental results for the solubility and for the thermodynamic properties of solvation.

4. Conclusions

From the comparison between the present results for the solubility of isobutane in $[C_nC_1Im][NTf_2]$ ionic liquids and those, previously published of n-butane in the same ionic liquids, it was possible to understand how the structure of the solute affects the solvation mechanisms of apolar solutes in ionic liquids with variable apolar moieties.

Both isobutane and n-butane are quite soluble in the ionic liquids studied and their solubility increases with the increase of the size of the alkyl side-chain of the imidazolium cation in the bis(trifluoromethylsulfonyl)amide ionic liquids. Iso-butane is nevertheless significantly less soluble than n-butane in these ionic liquids and the difference can be explained, in great measure, by the difference in the enthalpy of solvation of the two solutes, as seen in figure 2. By using molecular simulation, evidence of the enthalpic effect that explains the increase of the solubility of isobutane as a function of the alkyl side-chain was also found by the analysis of the molecular structure of the solutions and of the different components of the potential interaction energies in the solutions.

Acknowledgement

V.B. acknowledges CONICYT for the PhD fellowship and CONICYT-BECAS CHILE for supporting the research visit to Blaise Pascal University in France. Support by FONDECYT through Grant 11090013, Financiamiento Basal Para Centros Cientıficos y Tecnologicos de Excelencia and also by Millennium Nucleus CILIS, Project ICM-P10-003-F is acknowledged.

References

[1] A.A.H. Padua, M.F. Costa Gomes, J.N. Canongia Lopes, Acc. Chem. Res. 40 (2007) 1087.
[2] M.F. Costa Gomes, J.N. Canongia Lopes, A.A.H. Padua, Top. Curr. Chem. 290 (2009) 161.
[3] M.F. Costa Gomes, L. Pison, A.S. Pensado, A.A.H. Padua, Faraday Disc. 154 (2012) 41.
[4] L. Pison, J.N. Canongia Lopes, L.P.N. Rebelo, A.A.H. Padua, M.F. Costa Gomes, Phys. Chem. B 112 (2008) 12394.
[5] A. Bonhote, A.P. Dias, N. Papageorgiou, K. Kalyanasundaram, M. Gratzel, Inorg. Chem. 35 (1996) 1168.
[6] L. Moura, M. Mishra, V. Bernales, P. Fuentealba, A.A.H. Padua, C.C. Santini, M.F. Costa Gomes, Phys. Chem. B 117 (2013) 7416.
[7] J. Jacquemin, M.F. Costa Gomes, P. Husson, V. Majer, Chem. Thermodyn. 38 (2006) 490.
[8] J. Jacquemin, P. Husson, V. Majer, M.F. Costa Gomes, Fluid Phase Equilib. 240 (2006) 87.
[9] W.F. Smith, T.R. Todorov, The DL_POLY molecular simulation package, 2.20, STFC Daresbury Laboratorys, Warrington, UK, 2007.
[10] W.L. Jorgensen, D.S. Maxwell, J. Tirado-Rives, Am. Chem. Soc. 118 (1996) 11225.
[11] J.N. Canongia Lopes, A.A.H. Padua, Phys. Chem. B 108 (2004) 16893.
[12] J.N. Canongia Lopes, J. Deschamps, A.A.H. Padua, Phys. Chem. B 108 (2004) 2038.
[13] G. Kaminski, W.L. Jorgensen, Phys. Chem. 100 (1996) 18010.
[14] J.H. Dymond, E.B. Smith, The Virial Coefficients of Pure Gases and Mixtures, Clarendon Press, Oxford, 1980.
[15] D. Camper, C. Becker, C. Koval, R. Noble, Ind. Eng. Chem. Res. 44 (2005) 1928.